Available online at www.sciencedirect.com
SCIENCE DIRECT®
Catalysis Today 102–103 (2005) 177–182
CATALYSIS TODAY
www.elsevier.com/locate/cattod

Promotion by a second metal or SO_2 over vanadium supported on mesoporous carbon-coated monoliths for the SCR of NO at low temperature

E. García-Bordejé [a,*], A. Monzón [b], M.J. Lázaro [a], R. Moliner [a]

[a] *Instituto de Carboquímica (C.S.I.C), Miguel Luesma Castán 4, 50015 Zaragoza, Spain*
[b] *Departamento de Ingeniería Química y Tecnologías del medioambiente, Facultad de ciencias, Universidad de Zaragoza, Pedro Cerbuna 12, 50009 Zaragoza, Spain*

Available online 21 March 2005

Abstract

This work presents the promoting effects of the addition of a second metal to the catalyst and of the addition of SO_2 to the feed during the SCR of NO with ammonia at low temperature over vanadium supported on carbon-coated monoliths. Comparing both effects, the addition of SO_2 in the feed is a much more effective promoter that the addition of a second metal to vanadium. Upon introduction of 400 ppm SO_2 there is around a three-fold increase in the specific activity of the catalyst. It was found that mesoporosity of carbon support plays a key role on the durability of the promoting effect of SO_2 at low temperatures.

Keywords: Carbon-coated monoliths; Mesoporous carbon; Vanadia catalyst; SCR of NO

1. Introduction

The best available technology for reducing nitrogen oxide emissions from stationary sources is the selective catalytic reduction (SCR) of NO_x by ammonia. The industrial operations are carried out on $V_2O_5 + WO_3$ (MoO_3)/TiO_2 catalysts at 573–673 K [1]. However, the high concentration of SO_2 and ash in the flue gas reduces their performance and longevity. To circumvent this problem, an attractive option is to place the SCR unit downstream of the desulfurizer and electrostatic precipitators where most SO_2 and ash have been removed. Since the temperature in the downstream is typically below 473 K, it is necessary the development of low temperature SCR catalysts to avoid reheating of the flue gas and thus decreasing the cost of the process. Even after the desulfurizer ca. 100–400 ppm SO_2 remains that can still deactivate titania-supported vanadia at temperatures lower than 573 K. Catalysts supported on carbon have shown very high activity at low temperature and resistance to the remaining SO_2. Different metal oxides have been supported on carbon, e.g. V [2–6], Fe [7,8], Mn [9,10], Cu [8,11]. Vanadium oxide is one of the most active and resistant to SO_2. Moreover, its activity is reported to be promoted when SO_2 is present in the feed [3–5].

In this work, a novel monolithic catalyst based on vanadium supported on mesoporous carbon has been prepared and tested in the SCR of NO at low temperature (393–453 K). We have studied the promotion by the addition of a second metal with proved activity in the SCR of NO, viz. Fe, Cr, Cu and Mn. We have also investigated the enhanced activity when SO_2 is present in the feed.

2. Experimental

Cordierite monoliths (62 cm^{-2}) were coated with a mesoporous carbon derived from a polymer blend by the dipcoating method [12,13]. The polymers used are Furan resin (Huttenes-Albertus) and polyethylene glycol—6000 m.wt. (Sigma-Aldrich). Oxygenated surface groups were

* Corresponding author. Tel.: +34 976733977; fax: +34 976733318.
E-mail address: jegarcia@carbon.icb.csic.es (E. García-Bordejé).

0920-5861/$ – see front matter © 2005 Elsevier B.V. All rights reserved.
doi:10.1016/j.cattod.2005.02.026

created by immersing carbon-coated monoliths in a solution 2N of HNO_3 and stirring during 18 h at room temperature.

The catalyst impregnation was carried out by ion exchange of the cationic precursors with the protons of the functional groups of carbon support. This renders a uniform distribution of the catalyst along the monolith channels. The vanadium catalyst was prepared from ammonium metavanadate. After adding oxalic acid to solubilize metavanadate, vanadium is present in aqueous solution as VO_2^+. In the case of the bimetallic catalysts, the additive metal was impregnated from nitrate precursor after vanadium deposition. After impregnation the catalyst was rinsed with distilled water and dried first at room temperature and subsequently at 383 K. Finally, the catalyst was calcined in Ar at 673 K during 3 h.

The bimetallic catalysts were tested in the selective catalytic reduction of NO with ammonia at three temperatures 393, 423, 453 K. The gas composition was 700 ppm NO, 800 ppm NH_3, 3% O_2 and Ar to balance. The total amount of carbon coating was around 0.24 g and the total flow rate was 100 ml/min STP that yields a GHSV—17,000 h^{-1}. To analyse the gases, a mass spectrometer (Balzels) was used and the fragmentation pattern was dealt with as described previously [13].

To study the effect of the addition of SO_2 in the feed, a catalyst with 3% vanadium was tested at three temperatures, i.e. 393, 423, 453 K, with and without SO_2. The total flow rate was 100 ml/min STP and the amount of sample was around 0.15 g of carbon that yields a GHSV—34,000 h^{-1}. The gas composition was 500 ppm NO, 600 ppm NH_3, 3% O_2 and Ar to balance. When 400 ppm SO_2 was introduced the Ar flow rate was diminished to keep the same total flow rate, and therefore, the same concentration of reactants.

The bimetallic catalysts were characterized by TPR in a thermobalance CI Electronics Limited (UK), MK2 vacuum head model. The sample was heated up to 1073 K at a heating rate of 10 K/min. The total flow rate was 250 ml N/min with a composition of 40% H_2 and Ar to balance.

Temperature programmed desorption of preadsorbed NH_3 was carried out in a quartz microreactor. First the sample was pretreated with Ar up to 673 K to remove any adsorbed species. This step was omitted in samples after reaction with SO_2 to prevent the decomposition of sulphate salts. Then the temperature was set at 373 K and NH_3 was adsorbed on the catalyst at this temperature by allowing to flow 50 ml/min of 1800 ppm NH_3 in Ar during 2 h. Subsequently, the catalyst was treated with 50 ml/min of Ar during 1 h to remove the weakly adsorbed NH_3. Finally, the temperature was raised from 373 to 773 K at a heating rate of 10 K/min in 50 ml/min Ar. In the case of the samples after reaction with SO_2, the temperature was raised up to 1073 K. The desorption of NH_3 and SO_2 were followed by *m/e* 17 and 64, respectively, in the mass spectrometer.

3. Results and discussion

In a previous work [13], vanadium on carbon-coated monoliths with different loadings were prepared and characterized. The characterization showed that vanadia is well dispersed up to 6 wt.% loading. Since the loading of all the catalysts tested in this work is lower than 4 wt.%, the metal must be well dispersed. In all the experiments reported in this work, the selectivity to N_2 is around 100%.

3.1. Promotion by addition of a second metal

The reaction rate was found free of diffusional limitations [16]. Under these conditions and assuming first-order reaction with respect to NO (Table 1), the turnover frequency, i.e. number of moles of NO converted per mole of vanadium per second, can be calculated by the following equation:

$$\mathrm{TOF} = -\frac{F_0}{M}\ln(1-X) \quad (1)$$

where F_0 is the molar NO feed rate (mol/s), M is the moles of vanadium + moles of second metal and X is the conversion at steady state. The conversions and TOF values at 423 K of the catalyst here prepared are displayed in Table 1. The TOF values indicate that the SCR of NO is promoted by the addition of a second metal. To get some insight on the nature of this promotion, we characterized the catalysts by TPD of preadsorbed ammonia and TPR. The acidity of all the catalysts was probed by TPD of preadsorbed ammonia

Table 1
Bimetallic catalysts: turnover frequencies, parameter of Arrhenius equation and quantification of NH_3 desorbed in TPD of preadsorbed ammonia

Catalyst	k_o ($cm^3\ s^{-1}\ g^{-1}$)	E_a (kJ mol^{-1})	Conversion (%)	TOF at 423 K mol NO (mol metal[a])$^{-1}$ s^{-1} $\times 10^{-4}$	NH_3 desorbed m NH_3-TPD (mmol g^{-1})
3% V	227.9	13.9	43	1.6	0.070[b]
3% V–1% Fe	283.1	12.3	57	2.4	0.099
3% V–1% Mn	97.1	9.5	53	1.9	0.098
3% V–1% Cu	570.4	15.8	48	1.9	0.077
3% V–1% Cr	595.8	15.5	51	2.0	0.049

[a] Metal mol is the addition of the moles of vanadium and moles of the second metal.
[b] This values have been corrected for the desorption of the support.

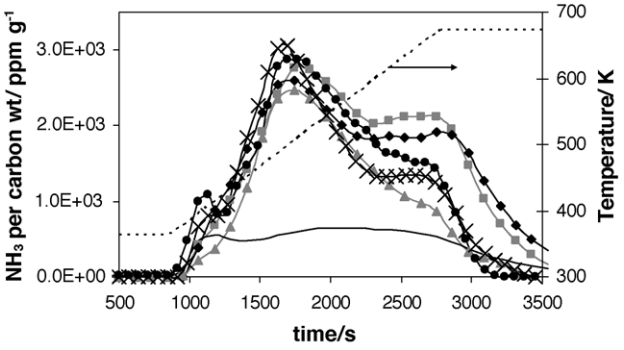

Fig. 1. Temperature programmed desorption of preadsorbed ammonia: (-) carbon support, (×) 3% V, (▲) 3 wt.% V–1 wt.% Cr, (■) 3 wt.% V–1 wt.% Fe, (●) 3 wt.% V–1 wt.% Cu, (◆) 3 wt.% V–1 wt.% Mn.

(Fig. 1). In the figure, it is apparent that the carbon support adsorbs some ammonia but the major part of acidity is due to the metal catalyst. Table 1 shows the quantification of desorbed ammonia. We looked for possible products of NH_3 oxidation (NO, N_2 and N_2O) and we did not find NO evolution ($m/e = 30$) in the temperature range of TPD experiments. However, we observed that $m/e = 28$ (N_2 or CO) and $m/e = 44$ (N_2O or CO_2) start to evolve at 623 and 573 K, respectively. Therefore, the shoulder in the NH_3-TPD at temperatures higher than 573 K is not fully reliable. On the other hand, at temperatures lower than 573 K, the desorption peaks give a true indication of the adsorbed ammonia since oxidation of NH_3 does not occur. Looking at the first NH_3 desorption peak at 500 K, all the catalyst do not show significant differences in acidity. Therefore, it is not possible to explain the differences in activity of the monometallic and bimetallic samples in base to differences in acidity.

Fig. 2 shows the results of TPR experiments. The maximum reduction rate occurs at about 100 K lower temperature in the bimetallic catalysts than in the monometallic catalyst. This superior reducibility of the bimetallic catalysts with respect to the monometallic catalyst can explain the enhanced activity by the addition of the second metal. The activation energies are different depending on the added metal suggesting that the nature of active sites changes with the added metal. The low apparent activation energy is typical of the SCR at low temperatures that is proposed to follow a Langmuir–Hinshelwood mechanism [14,15]. According to this mechanism the low activation energy would be the result of the exothermal contribution of adsorption and reoxidation vanadium to V^{5+}.

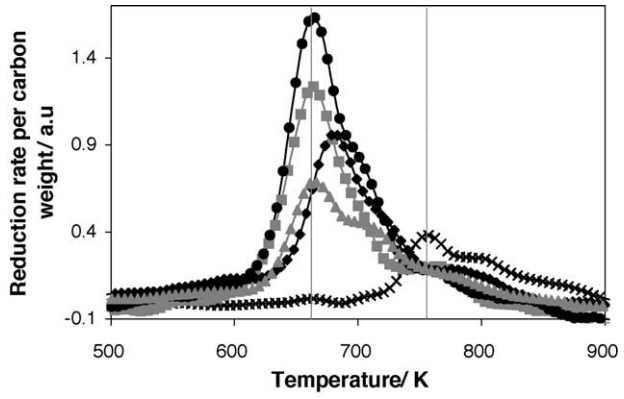

Fig. 2. Temperature programmed reduction of the bimetallic samples: (×) 3% V, (▲) 3 wt.% V–1 wt.% Cr, (■) 3 wt.% V–1 wt.% Fe, (●) 3 wt.% V–1 wt.% Cu, (◆) 3 wt.% V–1 wt.% Mn.

3.2. Promotion by SO_2 in the feed

As shown in Fig. 3, our catalyst is promoted when 400 ppm SO_2 is introduced in the feed regardless of the reaction temperature. The conversion is stable throughout the experiments (20 h time-on-stream) carried out at the two highest temperatures, i.e. 423 and 453 K. However, at 393 K there is a steady decay of conversion with time-on-stream. We calculated the turnover frequencies for the experiments in which the conversion is stable (Table 2). These TOF values undergo a three-fold increase upon addition of SO_2.

The promoting effect of SO_2 in the SCR of NO using vanadia supported on carbon has been widely studied by Zhu et al. [3–5]. These authors claim that the catalyst has to operate at temperatures above 473 K for the promoting role of SO_2 to occur and to be stable. Because they found that deactivation of the catalyst starts in 20 min at 423 K and in 4 h at 453 K after SO_2 introduction. They demonstrated that deactivation is due to the deposition of NH_4HSO_4.

It is apparent that our catalyst can operate steadily with SO_2 at lower temperature than those used by Zhu et al. The operation at the lowest temperature as possible increases the thermal efficiency by meeting the temperature of tail gas. The gas composition is the same as that used by Zhu et al. The main differences between their experiments and ours are the vanadium loading, the space velocity and the texture of both supports. Their catalyst has 0.6 wt.% V loading, while

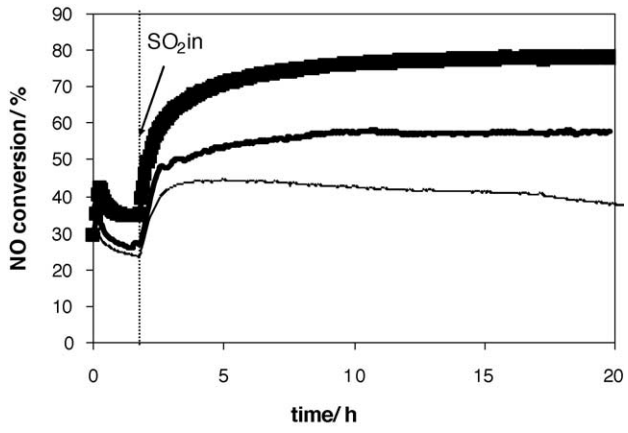

Fig. 3. Influence of the addition of SO_2 in the SCR of NO at three different temperatures. The thicker line correspond to higher temperature: (■) 453 K, (▬) 423 K, (—) 393 K. Composition of the gas: 500 ppm NO, 600 ppm NH_3, 3% O_2, Ar to balance (400 ppm SO_2 when added).

Table 2
Turnover frequencies at steady state before and after addition of 400 ppm SO_2 and quantification of the TPD (up to 1073 K) of preadsorbed ammonia

Reaction temperature	TOF (mol NO(mol V)$^{-1}$ s^{-1} × 10^{-4}		Quantification of TPD of preadsorbed ammonia		
	With fresh catalyst	20 h TOS with SO_2	mmol SO_2/g C	mmol NH_3/g C	NH_3/SO_2
423	1.7	4.9	2.74	6.53	2.13
453	4.9	9.6	2.02	5.95	2.64

ours has 3 wt.% V. Their experiments are carried out at 90.000 h^{-1}, while ours at 34.000 h^{-1}. They use almost three times higher space velocity but this is not enough to explain the dramatic difference in stability between both catalysts. Hence, the reason of the unlike behaviour has to be found in the different textural features of both carbon supports. The carbon support used by Zhu et al. is essentially microporous, the micropore volume representing 70% of total pore volume. Whereas our carbon support is predominantly mesoporous, since mesoporosity accounts for 80% of total pore volume.

The porosity of the samples after reaction with SO_2 at the three reaction temperatures was measured by N_2 physisorption (Table 3). We tried different evacuation temperatures from 373 to 573 before N_2 physisorption measurements and we did not observe increase of porosity at degassing temperatures lower than 400 K. This points out that ammonium sulphates in the pores are not decomposed during evacuation at these temperatures. In all the experiments here reported, 390 K was set as degassing temperature. Table 3 also shows the elemental analysis of S and N after each test. The N moles decrease with increasing temperature due to the lower NH_3 coverage at higher temperatures. On the other hand, S moles do not show a clear trend with temperature. At the highest temperature 353 K, where the NH_3 coverage is the lowest, the ratio of N moles to S moles is close to 1 suggesting that the predominant species is NH_4HSO_4. At 393 and 423 K, mixtures of NH_4HSO_4 and NH_4SO_4 are possible. By XPS, we found bands with binding energies at 168.3 eV (sulphate) and at 401.2 eV (NH_4^+) that also revealed the presence of ammonium sulphate salt.

Sample after reaction at 453 K exhibits similar textural parameters than the support pointing out that at this reaction temperature there is no significant pore plugging by ammonium sulphates. In catalyst after reaction at 423 K, the BET surface area and pore volume are significantly lower than those of the support. This decrease in textural parameters is due to the accumulation of ammonium sulphates. This decline of porosity is mainly due to a decrease in the micropore parameters since mesopore parameters remain without variation. This indicates that ammonium sulphates are accumulated preferentially in the micropores. Moreover, this decrease of the micropore volume does not affect the catalyst stability because 80% of total pore volume is mesoporosity. In catalyst after reaction at 393 K, there is a significant decrease of all the textural parameters both in the microporous and mesoporous range. This plugging of mesoporosity coincides with the steady decay of conversion. In this latter experiment, we withdrew sample after 5 h time-on-stream when the catalyst exhibits the maximum conversion, i.e. before deactivation has started. This intermediate sample also was characterized by N_2 physisorption. The textural parameters (Table 3) show that some microporosity has been plugged but mesoporosity is not plugged yet.

It is worth to note that in catalyst after reaction at 453 and 393 K there are similar amounts of S determined by elemental analysis. As we have seen above, at 393 K, significant pore plugging occurs but not at 453 K. This suggests that the pore plugging at the lower temperature is not due to a higher amount of sulphates but rather to a different location of sulphates at the two temperatures. At 393 K, bulk ammonium sulphates must be formed, likely in homogeneous phase, which plug the smaller pores. In contrast, at 453 K, most sulphates must be present as surface species that do not lead to significant pore plugging.

From the results above mentioned, some conclusions can be derived. First, it has been observed that the lower the reaction temperature the higher the accumulation rate of ammonium sulphate salts. In addition, the ammonium sulphate salts accumulate previously in the micropores and subsequently in the mesopores. When plugging of mesopores occurs, there is an ensuing decrease of conversion with TOS. We interpret the preferential accumulation in the

Table 3
Textural characterization by N_2 physisorption of samples after reaction with SO_2 at different temperatures

Sample	Total pore volume (cm^3 g^{-1})	Micropore area (m^2 g^{-1})	Mesopore area (m^2 g^{-1})	Micropore volume (cm^3 g^{-1})	Mesopore volume (cm^3 g^{-1})	Elemental analysis	
						SO_2 mmol/g C	NH_3 mmol/g C
Support	1.19	429	339	0.25	0.94	0	0
20 h TOS at 453 K	1.19	422	315	0.23	0.95	1.8	2.9
20 h TOS at 423 K	1.10	259	299	0.15	0.95	2.7	4.5
20 h TOS at 393 K	0.96	292	250	0.16	0.80	1.8	5.8
5 h TOS at 393 K	1.11	288	259	0.16	0.95	1.2	2.8

Composition of the gas: 500 ppm NO, 600 ppm NH_3, 3% O_2, 400 ppm SO_2, Ar to balance.

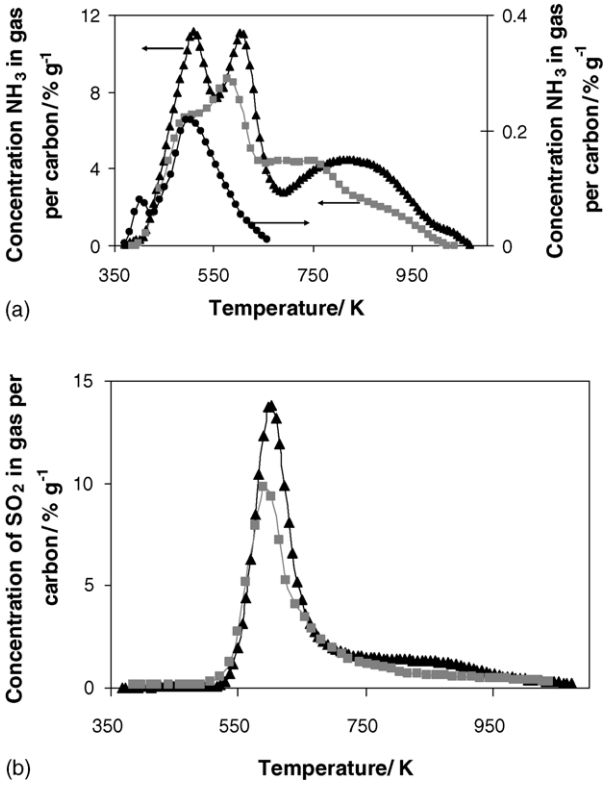

Fig. 4. Temperature programmed desorption of preadsorbed ammonia for catalyst after reaction with SO_2 at 423 and 453 K. (a) Desorption of NH_3: (●) fresh catalyst with 3% V, (▲) catalyst sulphated at 423 K, (■) catalyst sulphated at 453 K. (b) Desorption of SO_2: (▲) catalyst sulphated at 423 K, (■) catalyst sulphated at 453 K.

micropores because ammonium sulphates formed in the mesopores reacts readily with NO in the gas phase while ammonium sulphates formed in the micropores is less reactive leading to its accumulation. This lower reactivity in the micropores could be tentatively explained either because ammonium sulphates are more strongly retained due to the overlapping adsorption potential of the micropore walls or because of the lower accessibility to NO in gas phase.

TPD of preadsorbed ammonia was also carried out with catalyst after reaction with SO_2. For the sake of comparison, Fig. 4a shows the concentration of NH_3 desorbed in TPD of preadsorbed ammonia of catalyst after reaction with SO_2 at 423 and 453 K and that desorbed in fresh catalyst (3 wt.% V). In the sulphated catalyst the desorption of ammonia shows two peak with maximums at 518 and at 607 K. This latter peak coincides with the desorption of SO_2 (Fig. 4b) and, consequently, it is ascribed to the decomposition of ammonium sulphate salts. The first ammonia desorption peak is due to ammonia adsorbed on acid sites. The quantification of TPD is shown in Table 2. Comparing the amount of ammonia desorbed in the sulphated catalysts with that desorbed in the fresh catalyst (Table 1), it is apparent that the amount of ammonia desorbed in the sulphated catalyst is about two orders of magnitude higher than in the fresh catalyst. This indicates that after reaction with SO_2 a great amount of acid sites have been created. These sites

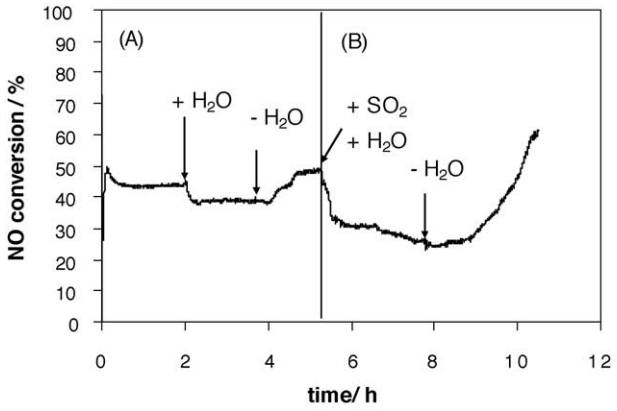

Fig. 5. Influence of the addition or removal of 5% H_2O in the feed at 473 K. (A) Feed gas composition: 500 ppm NO, 600 ppm NH_3, 3% O_2, Ar to balance. (B) The same gas composition as (A) + 400 ppm SO_2.

must be responsible of the promoted activity of the samples upon introduction of SO_2 in the feed.

Some preliminary experiments have been carried out studying the influence of the addition of 5% (v/v) H_2O vapour to the gas feed that is shown in Fig. 5. The introduction of H_2O depresses the NO conversion reversibly. This effect is attributed in the literature to the competitive adsorption of H_2O [17,18]. The inhibition is more pronounced when SO_2 is present in the gas feed and the promotion by SO_2 does not occur in the presence of water. Upon H_2O removal, the initial NO conversion is regained when SO_2 is not present in the feed, and when SO_2 is present, the conversion increases above the initial one because the promoting effect of SO_2 takes place. After introduction of H_2O the conversion decreases very fast but the response time is larger after H_2O removal.

4. Conclusions

The addition of a second metal resulted in a modest increase of the specific activity. Improvement of activity is attributed to the superior reducibility of the bimetallic catalyst with respect to the monometallic catalysts. The promoted activity of the bimetallic catalysts can not be explained in base to acidity since this is comparable in all the catalysts.

The other cause of promotion studied here is the addition of SO_2 in the feed. The specific activity is multiplied by a factor of three when SO_2 is introduced in the feed. This promoting effect is more pronounced than the addition of a second metal. In contrast with the literature, the activity is stable during at least 20 h operation both at 423 and 453 K. This is attributed to the role played by mesoporosity of our carbon support. At these temperatures, there is an accumulation of NH_3HSO_4 preferentially in the micropores that deactivates vanadia active phase located in this kind of pores. On the other hand, NH_3HSO_4 do not plug the

mesopores which are predominant in our carbon support (80% total pore volume). As a result of this, the enhanced activity of our catalyst is preserved during long-term testing.

Acknowledgments

Authors wish to thank Hüttenes-Albertus (Hannover) and Corning (New York) for supplying the Furan resin and cordierite monoliths, respectively. The authors are indebted to the Spanish Ministry of Science and Technology (PPQ-2002-02698 and BFM-2001-0209) and ''Gobierno de Aragón'' for the financial support. E. García-Bordejé acknowledges the Spanish government for a ''Ramón y Cajal'' contract. We are very grateful to M. Vijuesca and J.L. Pinilla for the assistance in the preparation of the monolithic catalysts and to T. Ubieto for carrying out the TPR experiments.

References

[1] H. Bosch, F. Janssen, Catal. Today 2 (1988) 369.
[2] S. Kasaoka, E. Sasaoka, H. Iwasaki, Bull. Chem. Soc. Jpn. 62 (1989) 1226.
[3] Z. Zhu, Z. Liu, H. Niu, S. Liu, J. Catal. 187 (1999) 245.
[4] Z. Zhu, Z. Liu, H. Niu, S. Liu, T. Hu, Y. Liu, Y. Xie, J. Catal. 197 (2001) 6.
[5] Z. Zhu, H. Niu, Z. Liu, S. Liu, J. Catal. 195 (2000) 268.
[6] T. Valdés-Solís, G. Marbán, A.B. Fuertes, Appl. Catal. B: Environ. 46 (2003) 261.
[7] T. Grzybek, H. Papp, Appl. Catal. B: Environ. 1 (1992) 271.
[8] J. Pasel, P. Kasner, M. Gazzano, A. Vaccari, W. Makowski, T. Lojewski, R. Dziembaj, H. Papp, Appl. Catal. B: Environ. 18 (1998) 199.
[9] T. Grzybek, J. Pasel, H. Papp, Phys. Chem. Chem. Phys. 1 (1999) 341.
[10] G. Marbán, R. Antuña, A.B. Fuertes, Appl. Catal. B: Environ. 41 (2003) 323.
[11] Z. Zhu, Z. Liu, S. Liu, H. Niu, T. Hu, T. Liu, Y. Sie, Appl. Catal. B: Environ. 26 (2000) 25.
[12] E. García-Bordejé, F. Kapteijn, J.A. Moulijn, Carbon 40 (2002) 1079.
[13] E. García-Bordejé, M.J. Lázaro, R. Moliner, J.F. Galindo, J. Sotres, A.M. Baró, J. Catal. 223 (2004) 395–403.
[14] G. Marbán, A.B. Fuertes, Catal. Lett. 84 (2002) 13.
[15] F. Kapteijn, L. Singoredjo, N.J.J. Dekker, J.A. Moulijn, Ind. Eng. Chem. Res. 32 (1993) 445.
[16] E. García-Bordejé, L. Calvillo, M.J. Lázaro, R. Moliner, Ind. Eng. Chem. Res. 43 (2004) 4073.
[17] M.D. Amiridis, I.E. Wachs, G. Deo, J.M. Jehng, D.S. Kim, J. Catal. 161 (1996) 247.
[18] W.S. Kijstra, J.C.M.L. Daamen, J.M. van de Graaf, B. van der Linden, E.K. Poels, A. Bliek, Appl. Catal. B: Environ. 7 (1996) 337.